

Virtual-element and multipoint finite-volume methods in Arcane's framework - Application to multi-physics CO₂ storage simulations

L. Agélas, G. Enchéry, I. Faille + teams of Arcane, ArcGeoSim, Alien and Geoxim

March 24th, 2025

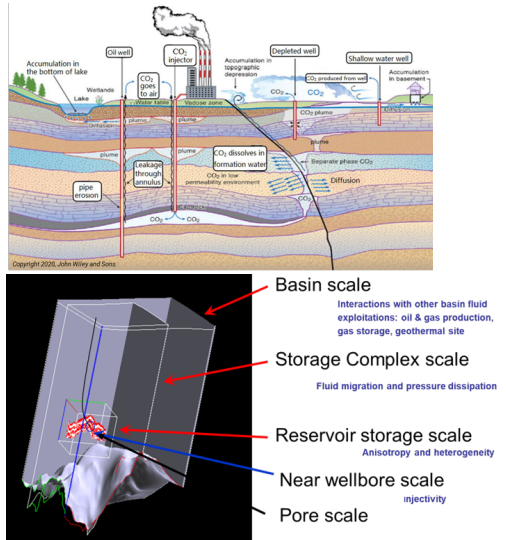
Arcane's days



Motivation/context - Numerical modelling of CO₂ storage

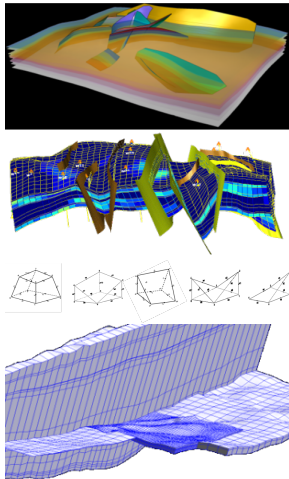
Need of a tool:

- to provide storage capacity estimates,
- to demonstrate storage integrity,
- to study and optimize injectivity,
- to be used in wider workflows with subsurface and fluid characterizations, uncertainty quantifications and monitoring of the storage.
- which is **multiscale**,
 - * in space (CO₂ plume scale ≪ Pressure variations ≪ stress perturbations scale (> 100 km)),
 - * and in time (from minutes to several thousand years).
- **multi-physics** : coupled THMC processes
 - * TH : Compositional multiphase flow and thermal transfers (CO₂ plume migration, dissolution)
 - * C : Fluid-rock interactions (mineral trapping, injectivity issues)
 - * M : Mechanical deformation (storage integrity)
 - + Surface deformation
 - + Avoiding fracturation, faults reactivation



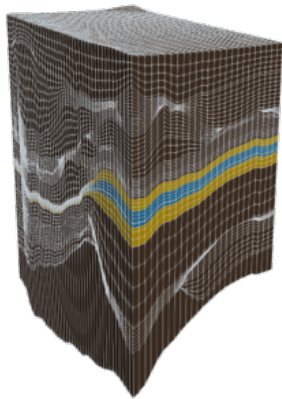
Grids for field scale simulations

- Subsurface characteristics:
 - * heterogeneous, multiscale,
 - * elongated domains composed of stratified geological layers,
 - * discontinuous (faults)
- Standard geoscience grids : Corner Point Geometry (CPG) grids
 - * built according to the geological layers,
 - * based on pillars, placed on a lateral grid, that follow the main faults,
 - * hexahedra and degenerated hexahedra, potentially very elongated cells,
 - * non-matching :
 - + across fault surfaces,
 - + nested locally refined grids to account for the different scales that need to be captured.
 - * CPG grids often require some of the faults to be stair-stepped which is not compatible with mechanical modeling of faults,
 - * **There is still a need for more flexible grids.**



Coupling flow and mechanics on geoscience grids

- Approach originally developed for studies :
 - * external coupling of FV fluid-flow simulator with a FE structural mechanics code (Code_Aster using Q1 FE),
 - * provides direct access to advanced constitutive laws (e.g. elastoplasticity),
 - * CPG degenerated hexahedra not compatible with Q1 FE → modification of the grid.
- FV TPFA not accurate enough, MPFA not robust enough
- Proposed approach for poro-mechanical problems solved on a single grid
 - * **VEM** : seen as a way to perform mechanical computations directly on CPG grids without increasing the numerical complexity compared to Q1 FEM
 - * **Non Linear FV schemes** : better trade-off between accuracy and stability/robustness compared to TPFA/MPFA, in particular for non-matching grids, without introducing additional discrete unknowns



Outline

1. Finite-volume weighted one-sided flux approximations (WOS schemes)
WOS schemes for heterogeneous anisotropic diffusion on general meshes
Application to poroelasticity and coupling with the virtual element method

2. Use in Geoxim calculator

Outline

1. Finite-volume weighted one-sided flux approximations (WOS schemes)
WOS schemes for heterogeneous anisotropic diffusion on general meshes
Application to poroelasticity and coupling with the virtual element method
2. Use in Geoxim calculator

Steady heterogeneous diffusion problem (Schneider, Agélas, E., Flemisch, 17)

Ω a polygonal subset of \mathbb{R}^d . $\bar{\Lambda}(x)$ a symmetric diffusion tensor. First model problem:

$$\begin{aligned}-\nabla \cdot (\bar{\Lambda} \nabla \tilde{u}) &= f \text{ in } \Omega, \\ \tilde{u} &= 0 \text{ on } \partial\Omega,\end{aligned}\tag{1}$$

with $f \in L^2(\Omega)$.

For any cell $K \in \mathcal{T}$, the divergence formula leads to

$$\int_K f \, dx = - \int_{\partial K} \bar{\Lambda} \nabla \tilde{u} \cdot \mathbf{n} = - \sum_{\sigma \in \mathcal{E}_K} \int_{\sigma} \bar{\Lambda} \nabla \tilde{u} \cdot \mathbf{n}_{K,\sigma}$$

where \mathcal{E}_K is the set of all faces included in ∂K and $\mathbf{n}_{K,\sigma}$ the unit vector normal to σ , oriented outwards to K .

Two-point flux approximation

Let σ be a face between two cells K and L with centers \mathbf{x}_K and \mathbf{x}_L . $\bar{\Lambda}$ assumed to be piecewise constant in each cell. Taking

$$\Lambda_{K,\sigma} = \mathbf{n}_{K,\sigma} \cdot \bar{\Lambda}_K \mathbf{n}_{K,\sigma}, \quad (2)$$

Two-Point Flux Approximation (TPFA):

$$-\int_{\sigma} \bar{\Lambda}_K \nabla \tilde{u} \cdot \mathbf{n}_{K,\sigma} \approx F_{K,\sigma}(u) = \frac{\Lambda_{\sigma} |\sigma|}{d_{\sigma}} (u_K - u_L) \quad (3)$$

where $|\cdot|$ is the measure of an element (face, cell....), $d_{\sigma} = d_{K,\sigma} + d_{L,\sigma}$, $d_{K,\sigma}$ the distance of \mathbf{x}_K to σ and

$$\Lambda_{\sigma} = \frac{d_{\sigma} \Lambda_{K,\sigma} \Lambda_{L,\sigma}}{d_{L,\sigma} \Lambda_{K,\sigma} + d_{K,\sigma} \Lambda_{L,\sigma}}. \quad (4)$$

Weighted one-sided fluxes

Assuming a decomposition of the conormal in the form:

$$\bar{\Lambda}_K \mathbf{n}_{K,\sigma} = \sum_{\sigma' \in \mathcal{S}_{K,\sigma}} \alpha_{K,\sigma\sigma'} (\mathbf{x}_{\sigma'} - \mathbf{x}_K) \quad (5)$$

where $\mathcal{S}_{K,\sigma}$ gathers σ' , included in ∂K with $\alpha_{K,\sigma\sigma'} \neq 0$, linear fluxes, $\tilde{F}_{K,\sigma}$, are given by:

$$\tilde{F}_{K,\sigma}(u) = m_\sigma \sum_{\sigma' \in \mathcal{S}_{K,\sigma}} \alpha_{K,\sigma\sigma'} (u_K - I_{\sigma'} u) \quad (6)$$

where $I_{\sigma'} u$ is a trace approximation of u (defined later). If $\sigma = K|L$, conservative fluxes can be obtained taking

$$F_{K,\sigma}(u, u) = \mu_{K,\sigma}(u) \tilde{F}_{K,\sigma}(u) - \mu_{L,\sigma}(u) \tilde{F}_{L,\sigma}(u), \quad (7)$$

with $\mu_{K,\sigma}(u) \geq 0$, $\mu_{L,\sigma}(u) \geq 0$ and $\mu_{K,\sigma}(u) + \mu_{L,\sigma}(u) = 1$. AvgMPFA defined by taking $\mu_{K,\sigma}(u) = \mu_{L,\sigma}(u) = \frac{1}{2}$.

Decomposing the conormal

The decomposition (5) is not unique. One possible way is to solve the following optimization problem

$$\begin{aligned} \min_{\gamma \geq 0, \tilde{\alpha} \in \mathbb{R}^{|\mathcal{E}_K|}} \quad & \kappa\gamma + \sum_{\sigma' \in \mathcal{E}_K} \tilde{\alpha}_{\sigma'} \text{ subject to } \frac{\langle \bar{\Lambda} \rangle_K \mathbf{n}_{K,\sigma}}{|\langle \bar{\Lambda} \rangle_K \mathbf{n}_{K,\sigma}|} = \sum_{\sigma' \in \mathcal{E}_K} \tilde{\alpha}_{\sigma'} \frac{\mathbf{x}_{\sigma'} - \mathbf{x}_K}{|\mathbf{x}_{\sigma'} - \mathbf{x}_K|}, \\ & \sum_{\sigma' \in \mathcal{E}_K} \tilde{\alpha}_{\sigma'} \frac{|\langle \bar{\Lambda} \rangle_K \mathbf{n}_{K,\sigma}|}{|\mathbf{x}_{\sigma'} - \mathbf{x}_K|} \geq \delta, \quad -C_\alpha \leq -\gamma \leq \tilde{\alpha}_{\sigma'} \leq C_\alpha \end{aligned} \tag{8}$$

where δ, C_α are strictly positive, $\kappa > |\mathcal{E}_K|$, $\delta \ll 1$ and $C_\alpha \gg 1$.

Reconstruction of the trace

Use of the harmonic averaging operator defined, for $\sigma = K|L$, by

$$I_\sigma u = \omega_{K,\sigma} u_K + \omega_{L,\sigma} u_L, \quad (9)$$

with

$$\omega_{K,\sigma} = \frac{d_{L,\sigma} \Lambda_{K,\sigma}}{d_{L,\sigma} \Lambda_{K,\sigma} + d_{K,\sigma} \Lambda_{L,\sigma}}. \quad (10)$$

In the case where $\sigma \in \partial\Omega$, $I_\sigma u = \frac{1}{m_\sigma} \int_\sigma \tilde{u} ds$.

Nonlinear two-point flux approximation (NLTPFA)

Here, the weights do not depend on u_K and u_L . We set

$$\mu_{K,\sigma}(u) = \frac{|\lambda_{L,\sigma}(u)| + \epsilon}{|\lambda_{K,\sigma}(u)| + |\lambda_{L,\sigma}(u)| + 2\epsilon} \quad (11)$$

with

$$\lambda_{K,\sigma}(u) = m_\sigma \sum_{\sigma' \in S_{K,\sigma}} \sum_{\sigma' = K|M, M \neq L} \alpha_{K,\sigma\sigma'} \omega_{M,\sigma'} u_M, \quad (12)$$

and $0 < \epsilon \leq h_T \min_{\sigma \in \mathcal{E}} m_\sigma$. With these weights, the flux is

$$F_{K,\sigma}(u, u) = t_{K,\sigma}(u)u_K - t_{L,\sigma}(u)u_L - R_{K,\sigma}(u) \quad (13)$$

where $R_{K,\sigma}(u)$ is a remaining term such that

$$|R_{K,\sigma}(u)| \leq \epsilon.$$

If all $\alpha_{K,\sigma\sigma'} \geq 0$ and ϵ sufficiently small, at each Picard iteration, the matrix related to (13) is an M-matrix.

Nonlinear multi-point flux approximation (NLMPFA)

Let us write

$$\tilde{F}_{K,\sigma}(u) = \tilde{F}_{K,\sigma}^{(1)}(u) + \tilde{F}_{K,\sigma}^{(2)}(u)$$

with $\beta_\sigma = \min(\alpha_{K,\sigma\sigma}\omega_{L,\sigma}, \alpha_{L,\sigma\sigma}\omega_{K,\sigma})$ and $\tilde{F}_{K,\sigma}^{(1)}(u) = m_\sigma \beta_\sigma (u_L - u_K)$. The weights are defined by

$$\mu_{K,\sigma}(u) = \mu_{L,\sigma}(u) = 0.5, \text{ if } \tilde{F}_{K,\sigma}^{(2)}(u) = \tilde{F}_{L,\sigma}^{(2)}(u) = 0, \quad \mu_{K,\sigma}(u) = \frac{|\tilde{F}_{L,\sigma}^{(2)}(u)|}{|\tilde{F}_{K,\sigma}^{(2)}(u)| + |\tilde{F}_{L,\sigma}^{(2)}(u)|}, \text{ otherwise.}$$

The non-linear flux is then given by:

$$F_{K,\sigma}(u, u) = \tilde{F}_{K,\sigma}^{(1)}(u) + \mu_{K,\sigma}(u) \left(1 - \operatorname{sign} \left(\tilde{F}_{K,\sigma}^{(2)}(u) \tilde{F}_{L,\sigma}^{(2)}(u) \right) \right) \tilde{F}_{K,\sigma}^{(2)}(u). \quad (14)$$

If all $\alpha_{K,\sigma\sigma'} \geq 0$, discrete maximum principles are satisfied.

Numerical analysis

Generic discrete problem defined over $\mathbb{P}_{\mathcal{T}}(\Omega)$ (space of piecewise constant function in each cell $K \in \mathcal{T}$):

$$\text{Find } u \in \mathbb{P}_{\mathcal{T}}(\Omega) \text{ s.t. } a_{\mathcal{T}}(u, u, w) = \int_{\Omega} fw \, dx \text{ for all } w \in \mathbb{P}_{\mathcal{T}}(\Omega) \quad (15)$$

where:

$$a_{\mathcal{T}}(u, v, w) = \sum_{K \in \mathcal{T}} \sum_{\sigma \in \mathcal{E}_K} F_{K,\sigma}(u, v) w_K. \quad (16)$$

Assuming that $a_{\mathcal{T}_n}$ is uniformly coercive (independently of n)

$$\forall (u, v) \in \mathbb{P}_{\mathcal{T}_n}(\Omega) \times \mathbb{P}_{\mathcal{T}_n}(\Omega), \quad a_{\mathcal{T}_n}(u, v, v) \gtrsim \|v\|_{\mathcal{T}_n}^2, \quad (17)$$

with $\|\cdot\|_{\mathcal{T}}$ a discrete H^1 -norm, one can show that

- problem (15) admits at least one solution,
- for a sequence of meshes, $\{\mathcal{T}_n\}_{n \in \mathbb{N}}$, s.t. $h_{\mathcal{T}_n} \rightarrow 0$ as $n \rightarrow \infty$, the sequence $\{u_n\}_{n \in \mathbb{N}}$ converges towards the weak solution \bar{u} to (1).

Assembling inner fluxes with automatic differentiation

```
m_matrixBuilder = [this](ArcNum::Vector &residual, ArcNum::Matrix &jacobian) {
    residual = 0.;

    _addSourceTerms(residual);

    const Arcane::Integer maxStencilSize = static_cast<Arcane::Integer>(m_stencil.get()->maxSize());
    const auto varU =
        Law::contribution<ScalarModel::U>(*m_varCellFolder, m_funcs, maxStencilSize,
                                             m_propVec, m_system);

    ENUMERATE_FACE(iFace, mesh()->innerActiveFaces()) {
        Law::initContribution();

        const auto isBackCellOwn(iFace->backCell().isOwn());
        const auto isFrontCellOwn(iface->frontCell().isOwn());

        if (isBackCellOwn || isFrontCellOwn) {
            m_stencil->init(iFace);

            Law::Contribution flux(0.);
            Law::Contribution downwardsGradFactor(options()->downwardsGradientFactor());
            m_scheme->computeFlux(*iFace, varU, *m_dirichletBC, flux, &downwardsGradFactor);

            if (isBackCellOwn) {
                const Law::Cell lawBackCell = m_stencil->backBoundaryCell();

                residual[0][lawBackCell] += flux;
                jacobian[0][lawBackCell][m_stencil] += flux;
            }

            if (isFrontCellOwn) {
                const Law::Cell &lawFrontCell = m_stencil->frontCell();

                residual[0][lawFrontCell] -= flux;
                jacobian[0][lawFrontCell][m_stencil] -= flux;
            }
        }

        m_stencil->finalize();
    }
}
```

Figure: Code sample in ArcaneDemo

Example

$f = 0$, $u = 10^5$ on the inner boundary,
 $u = 0$ on the outer one (see Figure on
the right).

$$\bar{\Lambda} = \mathbf{R}\left(\frac{\pi}{6}\right) \begin{pmatrix} 1000 & 0 \\ 0 & 1 \end{pmatrix} \mathbf{R}^{-1}\left(\frac{\pi}{6}\right)$$

with $\mathbf{R}(\alpha)$ the rotation matrix of angle
 α .

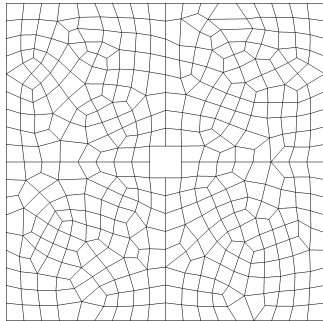


Figure: Used grid with hole
in the middle

Example

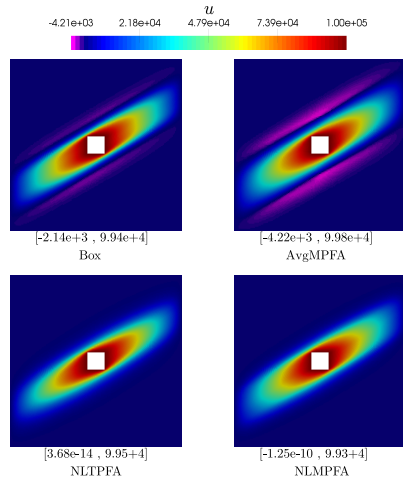


Figure: Solutions obtained with the Box, AvgMPFA, NLTPFA and NLMPFA schemes

Outline

1. Finite-volume weighted one-sided flux approximations (WOS schemes)
WOS schemes for heterogeneous anisotropic diffusion on general meshes
Application to poroelasticity and coupling with the virtual element method
2. Use in Geoxim calculator

Poroelasticity and coupling with VEM (E.,Agélas,23)- Model problem

$$-\nabla \cdot (\bar{\sigma}^e(\mathbf{u}) - \alpha p \bar{I}_d) = \mathbf{f}, \quad (18)$$

$$\partial_t(c_0 p + \alpha \nabla \cdot (\mathbf{u})) - \nabla \cdot (\bar{\Lambda}(\nabla p - \rho \mathbf{g})) = q \quad (19)$$

where $\bar{\sigma} = \bar{\sigma}^e(\mathbf{u}) - \alpha p \bar{I}_d$ the total stress, $\bar{\sigma}^e(\mathbf{u})$ Terzaghi's effective stress,

$$\bar{\sigma}^e(\mathbf{u}) = 2\mu \bar{\varepsilon}(\mathbf{u}) + \lambda \nabla \cdot (\mathbf{u}) \bar{I}_d, \quad \bar{\varepsilon}(\mathbf{u}) := \frac{1}{2}(\nabla \mathbf{u} + \nabla \mathbf{u}^T) \quad (20)$$

(μ, λ) are the Lamé coefficients, \mathbf{u} the rock displacement vector, α Biot-Willis' coefficient, \mathbf{f} a volumetric force, $c_0 > 0$ the product of porosity by the fluid compressibility. Associating to \mathbf{u}, p the indices d and p , setting $\partial\Omega = \Gamma_{D_\alpha} \cup \Gamma_{N_\alpha}$ for $\alpha \in \{d, p\}$:

$$\mathbf{u} = 0 \text{ on } \Gamma_{D_d}, \quad (21)$$

$$(\bar{\sigma}^e(\mathbf{u}) - \alpha p \bar{I}_d) \cdot \mathbf{n} = \mathbf{t} \text{ on } \Gamma_{N_d}, \quad (22)$$

$$p = 0 \text{ on } \Gamma_{D_p}, \quad (23)$$

$$\bar{\Lambda}(\nabla p - \rho \mathbf{g}) \cdot \mathbf{n} = \Phi \text{ on } \Gamma_{N_p}. \quad (24)$$

Initially,

$$p(\mathbf{x}, 0) = p_0(\mathbf{x}) \text{ in } \Omega \quad (25)$$

and $\mathbf{u}_0 = \mathbf{u}(\mathbf{x}, 0)$ is chosen as the solution to (18)-(21)-(22) with $p = p_0$.

Linear VEM spaces

Discrete approximation space used for the approximation of \mathbf{u} , \mathbf{u}_T , defined by

$$V_T = \bigcup_{K \in \mathcal{T}} V_K$$

where

$$V_K = \left\{ \varphi \in (H^1(K))^d \mid \varphi \cdot \mathbf{e}_i \in V_{\text{scal}, K}, \forall i = 1, \dots, d \right\},$$

\mathbf{e}_i denotes one of the vectors of the canonical basis of \mathbb{R}^d . For any face or cell element γ , a projection π_γ of a basis function $\varphi \in V_{\text{scal}, K}$ onto $\mathbb{P}_1(\gamma)$ is given by

$$\pi_\gamma(\varphi(\mathbf{x})) = \langle \nabla \varphi \rangle_\gamma \cdot (\mathbf{x} - \bar{\mathbf{x}}) + \bar{\varphi}$$

where $\langle \nabla \varphi \rangle_\gamma = \frac{1}{m_\gamma} \int_\gamma \nabla \varphi$, $\bar{w} = \frac{1}{\text{card}(\mathcal{V}(\gamma))} \sum_{v \in \mathcal{V}(\gamma)} w(\mathbf{x}_v)$, $w \in \{\varphi, \mathbf{x}\}$ and $\mathcal{V}(\gamma)$ is the set of all vertices of γ . For instance, for $d = 3$, we first introduce, for all faces $\sigma \in \mathcal{E}$, the face approximation spaces

$$V_{\text{scal}, \sigma} = \left\{ \varphi \in H^1(\sigma) \mid \forall \gamma \in \partial\sigma, \varphi|_\gamma \in \mathbb{P}_1(\gamma); \varphi|_{\partial\sigma} \in C^0(\partial\sigma); \Delta\varphi \in \mathbb{P}_1(\sigma); \int_\sigma \pi_\sigma(\varphi) q = \int_\sigma \varphi q, \forall q \in \mathbb{P}_1(\sigma) \right\}$$

and, then, for all $K \in \mathcal{T}$, the cell approximation spaces

$$V_{\text{scal}, K} = \left\{ \varphi \in H^1(K) \mid \forall \sigma \in \partial K, \varphi|_\sigma \in V_{\text{scal}, \sigma}; \Delta\varphi = 0 \text{ in } K \right\}.$$

We finally define

$$V_{T,0} = \{ \varphi \in (H^1(\Omega))^d \mid \varphi \in V_T; \varphi(\omega) = \mathbf{0} \text{ if } \omega \in \mathcal{V}_{D_d} \}.$$

Discrete weak form

Discrete weak formulation related to problem (18)-(21)-(22)-(25): for all $\mathbf{v}_T \in V_{T,0}$ and $n \in \{0 \dots N+1\}$:

$$\sum_{K \in T} \left(a_T^K(\mathbf{u}_T^n, \mathbf{v}_T) - \int_K \alpha p_T^n \nabla \cdot (\mathbf{v}_T) - \int_K \mathbf{f}^n \cdot \mathbf{v}_T - \int_{\partial K \cap \Gamma_{N_d}} \mathbf{t}_N^n \cdot \mathbf{v}_T \right) = 0 \quad (26)$$

where

$$a_T^K(\mathbf{w}_T, \mathbf{v}_T) = \int_K \bar{\sigma}^e(\pi_K(\mathbf{w}_T)) : \bar{\epsilon}(\pi_K(\mathbf{v}_T)) + s_K(\mathbf{w}_T, \mathbf{v}_T), \quad (27)$$

$$s_K(\mathbf{w}_T, \mathbf{v}_T) = h_T^{d-2} \|\bar{\bar{C}}\|_\infty \sum_{v \in \mathcal{V}(K)} ((\mathbf{w}_T - \pi_K(\mathbf{w}_T)) \cdot (\mathbf{v}_T - \pi_K(\mathbf{v}_T))) (\mathbf{x}_v), \quad (28)$$

$\bar{\bar{C}}$ being the stiffness tensor computed from the Lamé coefficients.

Using a WOS finite-volume approximation of (19)-(23)-(24)-(25)

$$m_K D^{n+1} \left(c_0 p_K + \alpha \int_K \nabla \cdot (\mathbf{u}_D) \right) - \delta t^{(n+\frac{1}{2})} \sum_{\sigma \in \mathcal{E}_K} F_{K,\sigma}(p^{n+1}, p^{n+1}) = \delta t^{(n+\frac{1}{2})} \int_K q^{n+1}, \quad (29)$$

with $D^{n+1} p = p^{n+1} - p^n$.

Numerical analysis

Under a few assumptions, including that the solution (\mathbf{u}, p) to (18)–(25) is smooth enough and that $\delta t^{(n+\frac{1}{2})} \leq \frac{c_0}{2}$,

- + For each $n_0 \in \{0 \dots N + 1\}$, there is at least one discrete solution $(\mathbf{u}_T^{n_0}, p_T^{n_0})$ to (26)–(27)–(28)–(29),
- + These solutions satisfy the a priori error estimate

$$\left(\|\mathbf{u} - \mathbf{u}_T\|_{L^\infty(0, T; H^1(\Omega))}^2 + \|p - p_T\|_{L^\infty(0, T; L^2(\Omega))}^2 + \|p - p_T\|_{L^2(0, T; \mathbb{P}_T(\Omega))}^2 \right)^{\frac{1}{2}} \lesssim \delta t^{(n+\frac{1}{2})} + h_T. \quad (30)$$

In (30), the constant depends on the physical data of the problem, regularity constants of the mesh and $\partial_{tt}\mathbf{u}$ and $\partial_{tt}p$.

Numerical example

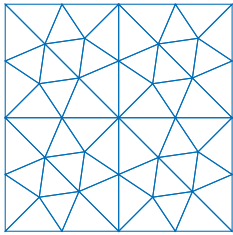
$\Omega = (0, 1)^2$, $T = 1$, Young modulus $E = 2.5$, poisson ratio $\nu = 0.25$, $\bar{\Lambda} = \bar{I}_d$, $\alpha = 1$, $c_0 = 0.5$ and

$$\mathbf{u}(\mathbf{x}, t) = 10^{-2} e^{-t} \begin{pmatrix} x^2 y \\ -x y^2 \end{pmatrix}, \quad (31)$$

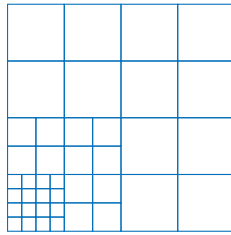
$$p(\mathbf{x}, t) = e^{-t} \sin\left(\frac{x}{\sqrt{2}}\right) \sin\left(\frac{y}{\sqrt{2}}\right). \quad (32)$$

Dirichlet conditions on the whole boundary $\partial\Omega$. Ω discretized with the grids `mesh1`, `mesh3` et `mesh4_1` (FVCA5 benchmark). For each grid, system (26)-(27)-(28)-(29) is solved with $\delta t^{(n+\frac{1}{2})} = 0.2, 0.1, 0.02, 0.01$.

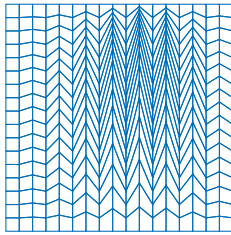
Grids



(a) `mesh1_1`



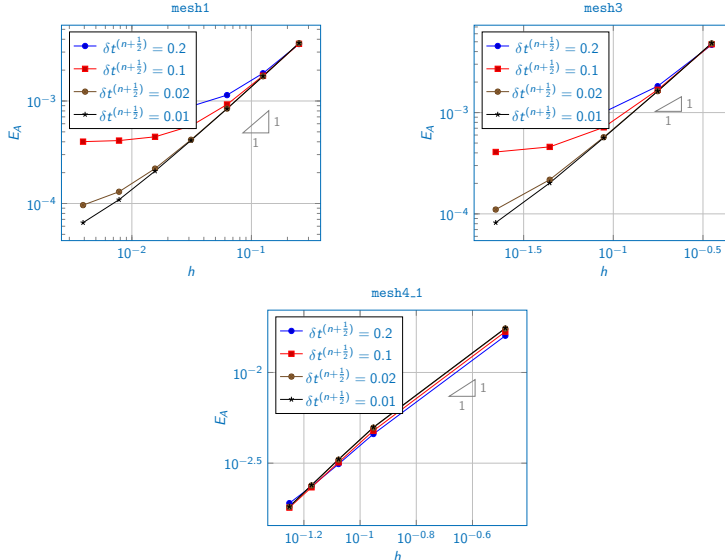
(b) `mesh3_1`



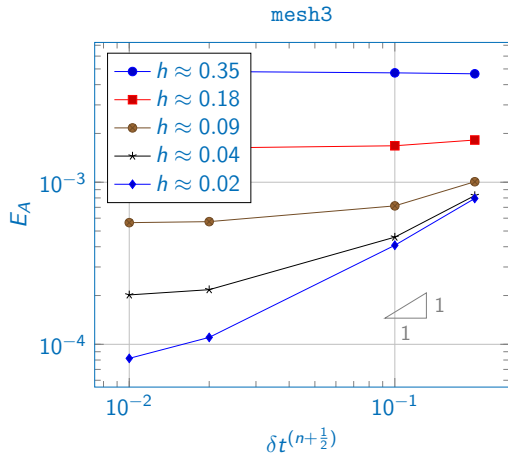
(c) `mesh4_1_1`

Figure: Coarsest level of the grid used for the convergence study

Space convergences with NLTPFA



Time convergence with mesh3 grids and NLTPFA



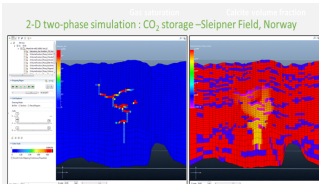
Outline

1. Finite-volume weighted one-sided flux approximations (WOS schemes)
WOS schemes for heterogeneous anisotropic diffusion on general meshes
Application to poroelasticity and coupling with the virtual element method

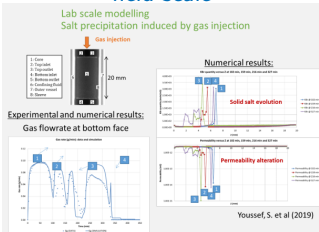
2. Use in Geoxim calculator

Numerical modeling for CO₂ storage: Geoxim calculator

- Research simulator:
 - * used in IFPEN for research studies or by partners through research collaborations,
- Initial focus on rock-fluid interactions (dissolution/precipitation of minerals) in addition to multi-phase compositional fluid flow:
 - * **flexible** physical system (species, components, phases) and physical laws



Water-gaz rock interactions at field scale

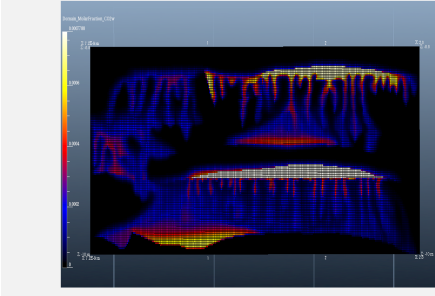


Study of coupled processes at laboratory scale

Numerical modeling for CO₂ storage: Geoxim calculator

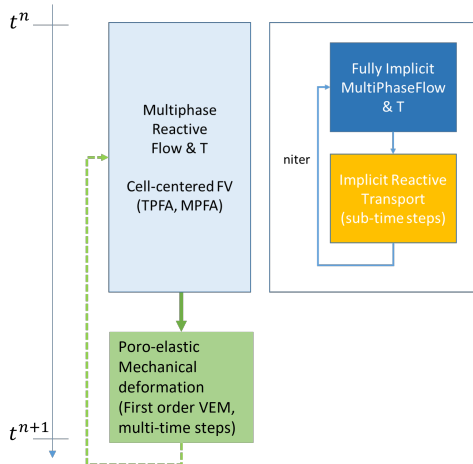
- Geoxim reactive multiphase flow capabilities:
 - * already available to study:
 - + trapping mechanisms : structural trapping, CO₂ dissolution, mineral trapping. . . ,
 - + injectivity : reactivity of injected fluids, porous medium alteration and loss of injectivity, drying and salt precipitation, hydrates formation . . . ,
 - * cell centered FV (TPFA/MPFA for diffusive fluxes),
 - * fully implicit multiphase flow,
 - * iterative coupling with implicit reactive transport
 - * challenge : robustness and efficiency in solving nonlinear algebraic equations
- Additional developments and improvements are still ongoing, mainly related to integrity study
 - * geomechanics,
 - * faults : flow, reactive transport and mechanics,

SPE11 comparative project <https://spe.org/csp>
Two-phase flow, Capillary trapping, CO₂ dissolution, gravity digitations



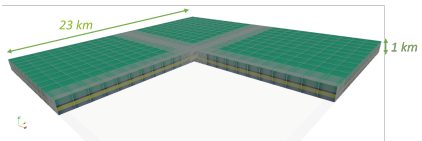
Geoxim: coupling flow and mechanics

- first order VEM
- multi-rate one-way coupling with flow & reactive transport:
 - * elastic properties evolve with porosity and mineral volume fractions (explicit)
- on-going work:
 - * multi-rate two-way coupling via the fixed stress algorithm.

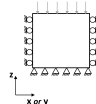
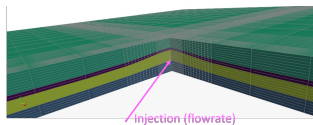


CO₂-water flow with NLTPFA and one-way coupling with VEM

- + Initial condition : water hydrostatic pressure, initial stress field (lithostatic, H/V stress ratios)
- + 20 years simulation, CO₂ injection for the first 10 years,
- + Slightly deformed scottish mesh, heterogeneous flow and elastic properties
- + Immiscible two-phase flow, no capillary pressures
- + Fully Implicit, NLTPFA derivatives in the Jacobian by means of automatic differentiation



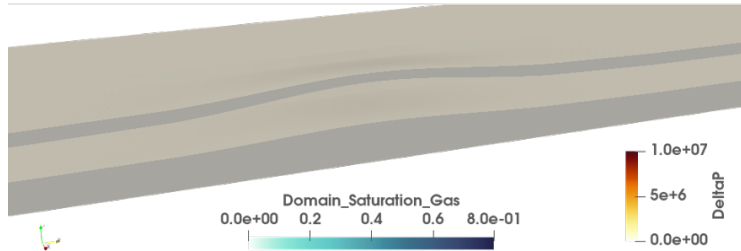
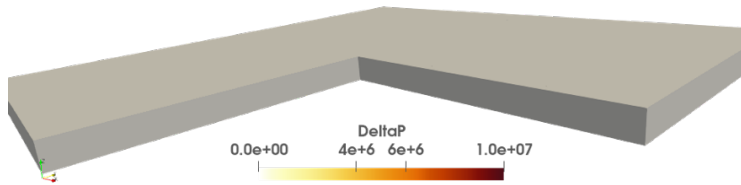
Overburden
Caprock
Aquifer
Underburden



CO₂-water flow with NLTPFA and one-way coupling with VEM

Time: 0.000000

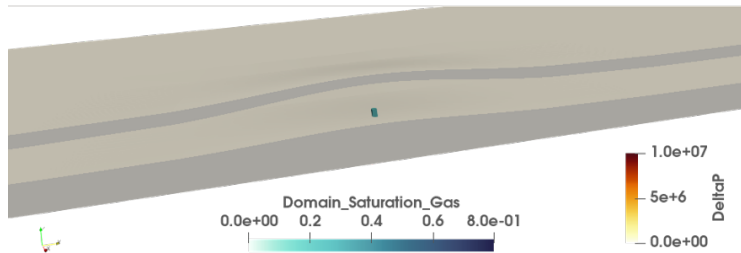
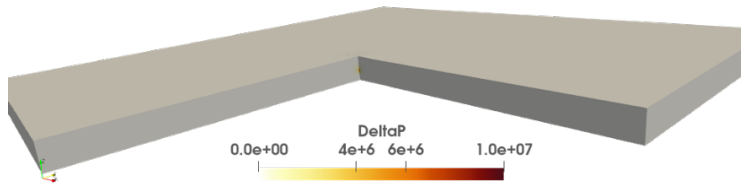
Deformed mesh with a scale factor of 50 000



CO₂-water flow with NLTPFA and one-way coupling with VEM

Time: 0.002000

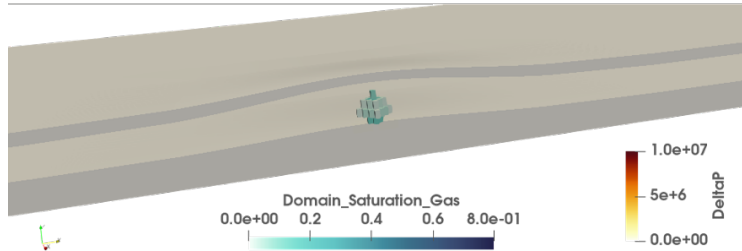
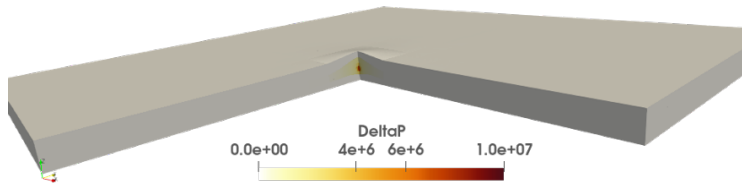
Deformed mesh with a scale factor of 50 000



CO₂-water flow with NLTPFA and one-way coupling with VEM

Time: 0.057000

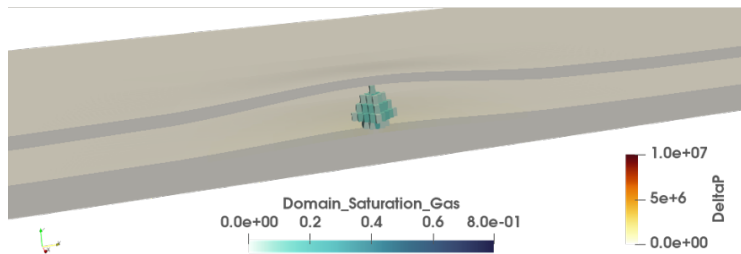
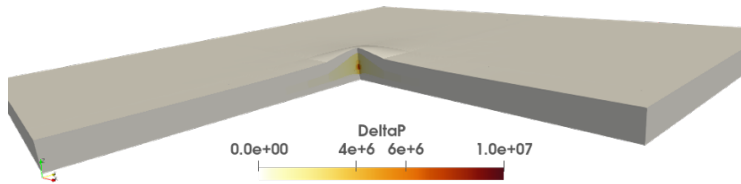
Deformed mesh with a scale factor of 50 000



CO₂-water flow with NLTPFA and one-way coupling with VEM

Time: 0.167000

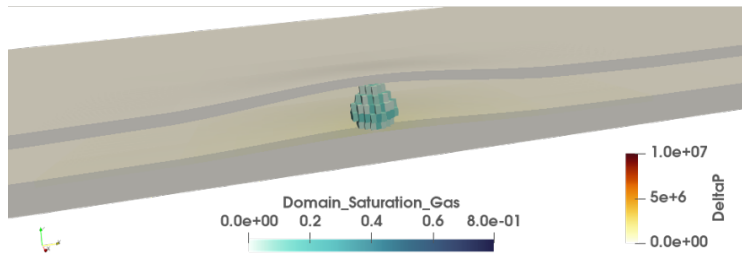
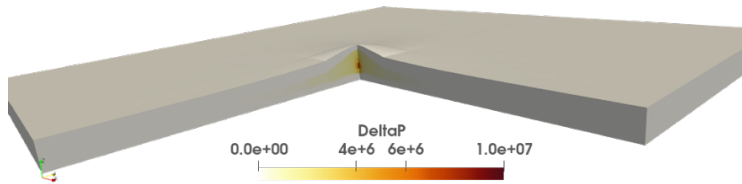
Deformed mesh with a scale factor of 50 000



CO₂-water flow with NLTPFA and one-way coupling with VEM

Time: 0.331000

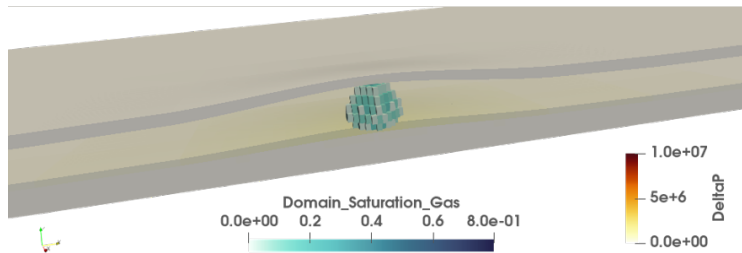
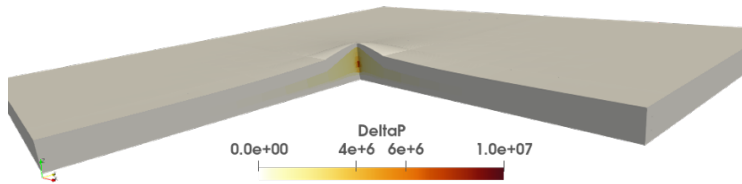
Deformed mesh with a scale factor of 50 000



CO₂-water flow with NLTPFA and one-way coupling with VEM

Time: 0.495000

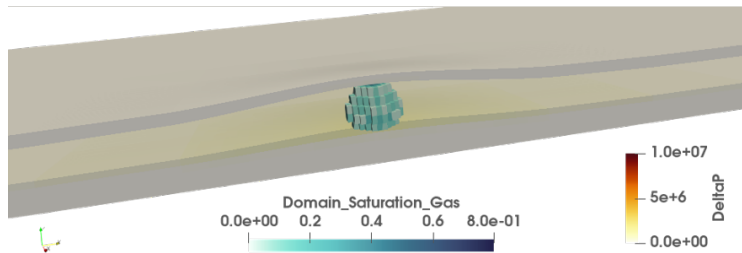
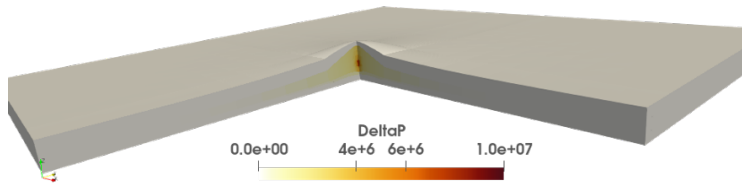
Deformed mesh with a scale factor of 50 000



CO₂-water flow with NLTPFA and one-way coupling with VEM

Time: 0.660000

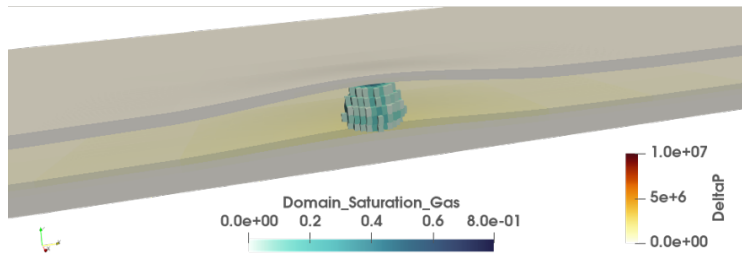
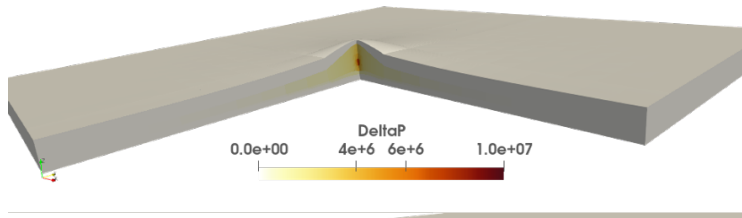
Deformed mesh with a scale factor of 50 000



CO₂-water flow with NLTPFA and one-way coupling with VEM

Time: 0.824000

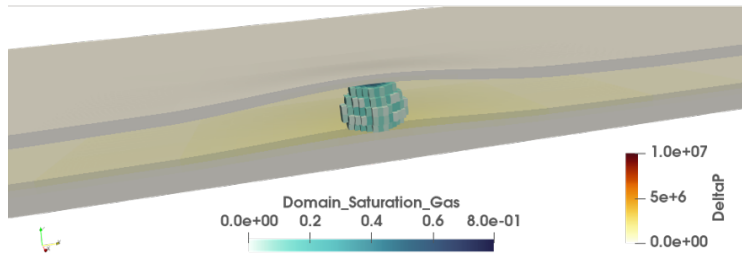
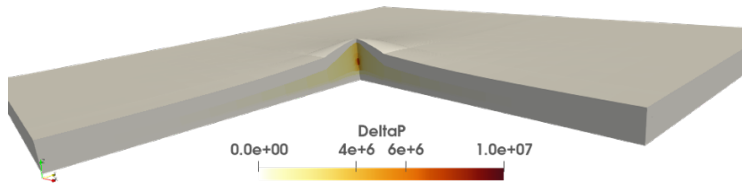
Deformed mesh with a scale factor of 50 000



CO₂-water flow with NLTPFA and one-way coupling with VEM

Time: 0.989000

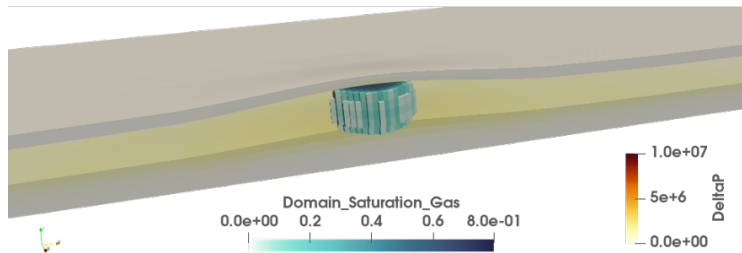
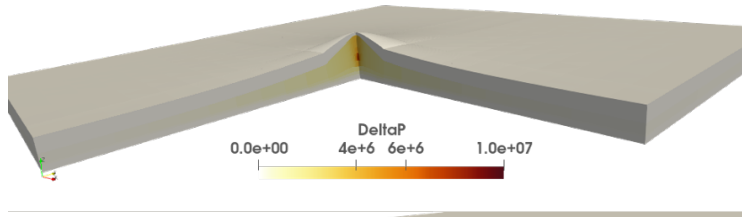
Deformed mesh with a scale factor of 50 000



CO₂-water flow with NLTPFA and one-way coupling with VEM

Time: 2.000000

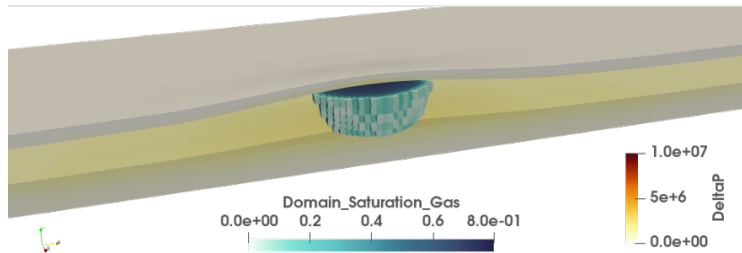
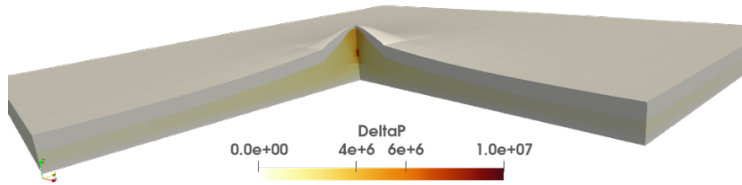
Deformed mesh with a scale factor of 50 000



CO₂-water flow with NLTPFA and one-way coupling with VEM

Time: 4.000000

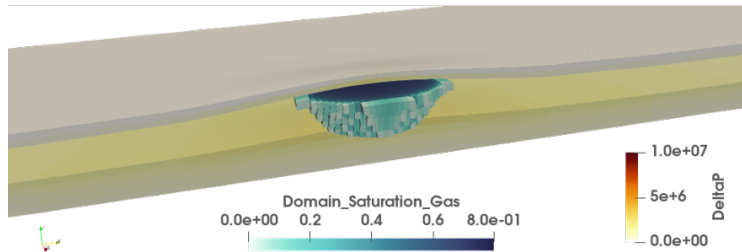
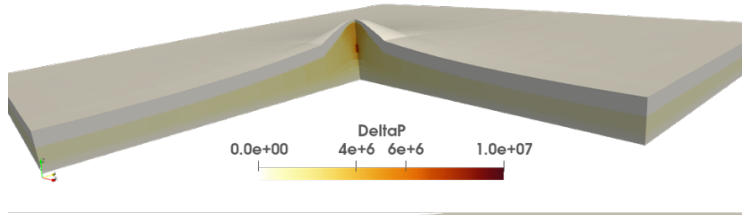
Deformed mesh with a scale factor of 50 000



CO₂-water flow with NLTPFA and one-way coupling with VEM

Time: 6.000000

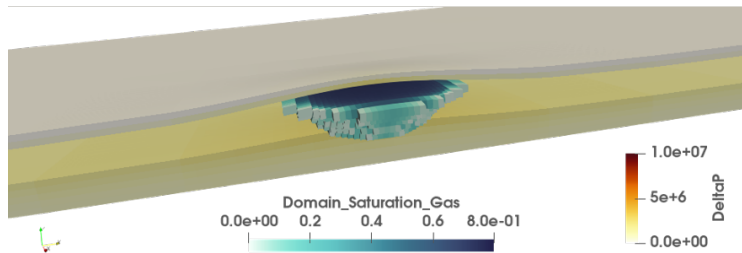
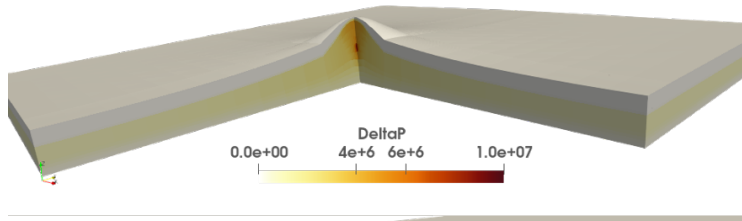
Deformed mesh with a scale factor of 50 000



CO₂-water flow with NLTPFA and one-way coupling with VEM

Time: 8.000000

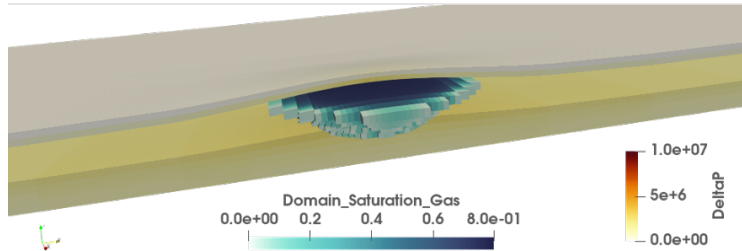
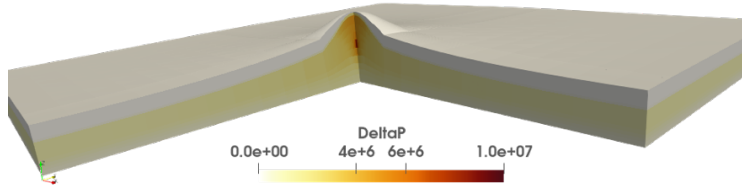
Deformed mesh with a scale factor of 50 000



CO₂-water flow with NLTPFA and one-way coupling with VEM

Time: 10.000000

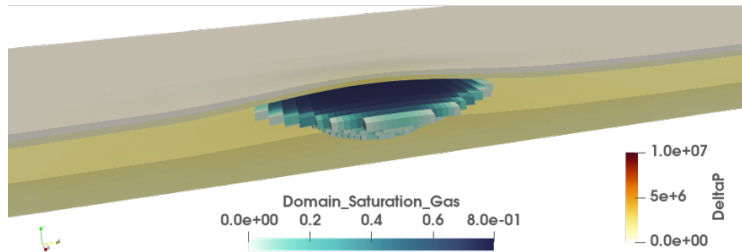
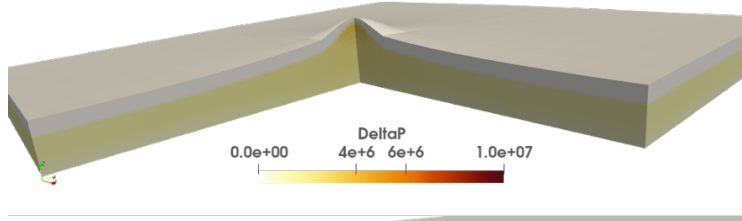
Deformed mesh with a scale factor of 50 000



CO₂-water flow with NLTPFA and one-way coupling with VEM

Time: 13.000000

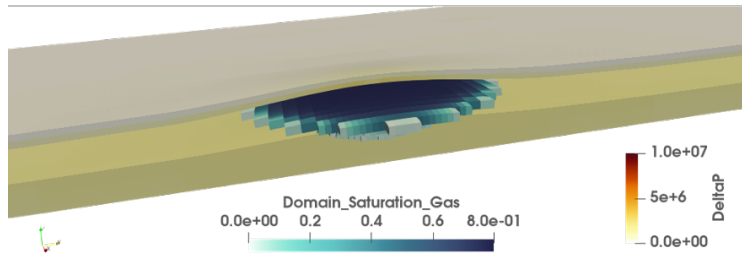
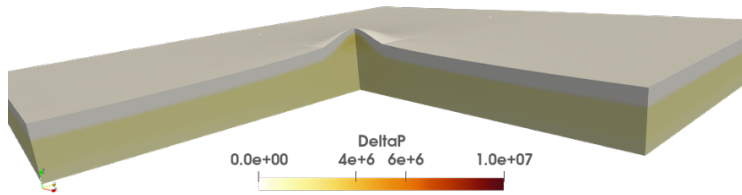
Deformed mesh with a scale factor of 50 000



CO₂-water flow with NLTPFA and one-way coupling with VEM

Time: 17.000000

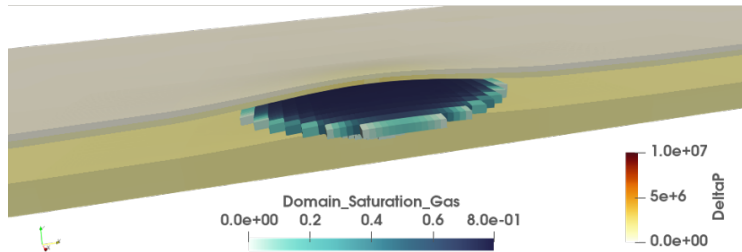
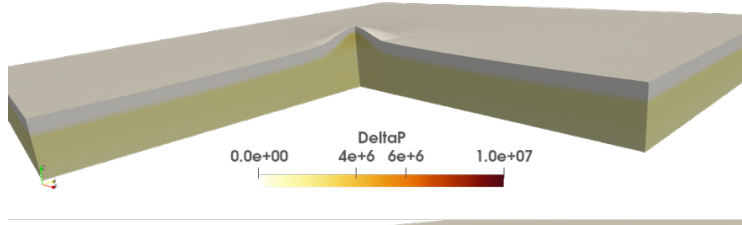
Deformed mesh with a scale factor of 50 000



CO₂-water flow with NLTPFA and one-way coupling with VEM

Time: 20.000000

Deformed mesh with a scale factor of 50 000



Conclusions/Perspectives

- + CO₂ storage:
 - * an application with unsatisfied grid/scheme needs for THMC simulations (stair-stepped faults with CPG grids, TPFA scheme not always consistent...)
- + but VEM coupled with NLTPFA/NLMPFA FV enable consistent HM computations on a single grid:
 - * on-going validation on more complex grids (LGR, not-matching),
 - * additional physics should be taken into account (fault contacts...).
- + on the mesh side:
 - * on-going study to transform CPG non-matching grids (with LGR and/or faults) into conforming polyhedral cells and to test them with the previous schemes.

Innovating for energy

Find us on:

🌐 www.ifpenergiesnouvelles.com

🐦 [@IFPENinnovation](https://twitter.com/IFPENinnovation)

